Helsinki University of Technology Institute of Mathematics Research Reports
Teknillisen korkeakoulun matematiikan laitoksen tutkimusraporttisarja
Espoo 2003 A456

A BENCHMARK STUDY OF ELLIPTIC AND HYPERBOLIC SHELLS OF REVOLUTION

Ville Havu Harri Hakula Tomi Tuominen

TEKNILLINEN KORKEAKOULU
TEKNISKA HÖGSKOLAN
HELSINKI UNIVERSITY OF TECHNOLOGY
TECHNISCHE UNIVERSITÄT HELSINKI
UNIVERSITE DE TECHNOLOGIE D'HELSINKI

Helsinki University of Technology Institute of Mathematics Research Reports
Teknillisen korkeakoulun matematiikan laitoksen tutkimusraporttisarja
Espoo 2003 A456

A BENCHMARK STUDY OF ELLIPTIC AND HYPERBOLIC SHELLS OF REVOLUTION

Ville Havu Harri Hakula Tomi Tuominen

Helsinki University of Technology
Department of Engineering Physics and Mathematics
Institute of Mathematics

Ville Havu, Harri Hakula, Tomi Tuominen: *A Benchmark Study of Elliptic and Hyperbolic Shells of Revolution*; Helsinki University of Technology Institute of Mathematics Research Reports A456 (2003).

Abstract: *We consider several benchmark cases for finite element analysis of shells. An elliptic and a hyperbolic shell of revolution over a range of thickness and different boundary conditions are presented and accurate deformation profiles and energies are calculated. Also the existence of boundary layers is demonstrated.*

AMS subject classifications: 74S05, 74K25

Keywords: shells, finite elements, benchmark

Ville.Havu@hut.fi

ISBN 951-22-6315-7
ISSN 0784-3143

Helsinki University of Technology
Department of Engineering Physics and Mathematics
Institute of Mathematics
P.O. Box 1100, 02015 HUT, Finland
email:math@hut.fi http://www.math.hut.fi/

1 Introduction

Finite element analysis of thin shell structures is known to be a task of many aspects. Quality of the discretized solution depends on several factors, e.g. the geometry and thickness of the shell, degree of the interpolating polynomials, the regularity of the mesh, and the applied load.

A good finite element scheme for shells must be able to successfully confront a whole spectrum of different situations: the problem of locking in the bending-dominated state should be circumvented and the membrane-dominated deformations captured. Further, the detection and resolution of several boundary layers is required.

At the moment there is no general and unified theory for how to design a good finite-element procedure for a general shell structure. Therefore the design of new shell elements, as well as the ongoing testing of already existing ones, is often reliant on the use of sets of benchmark problems. Unfortunately, the test sets used do not necessarily cover all the phenomena present in thin shells, but are rather a "traditional collection" of problems to which the solution (or some part of the solution) is known.

Our plan is to propose a series of benchmark problems illustrating characteristic aspects of thin shells and their finite element analysis (for similar ideas, see [1]). Throughout the series we examine different types of shells of revolution. This first paper focuses into the nature of some relatively simple elliptic and hyperbolic shells. Our analysis is carried out in the spirit of [3] where the parabolic case (i.e. a cylinder) was thoroughly treated.

The plan of this paper is as follows. In section 2 we present the shell model used in numerical calculations. In section 3 the actual benchmark cases are specified and the results are presented in section 4. A short discussion is provided in section 5.

2 The Shell Model

Throughout the paper we consider the dimensionally reduced model of Reissner and Naghdi. In this model the total energy of the shell is given by

$$\mathcal{F}(\underline{u}) = \frac{1}{2}\mathcal{A}(\underline{u},\underline{u}) - Q(\underline{u}) \tag{1}$$

where $\mathcal{A}$ represents the (possibly scaled) deformation energy, Q denotes the load potential and $\underline{u} = (u, v, w, \theta, \psi)$ is the vector of three translations and two rotations. The deformation energy is further split into bending, membrane and transverse shear energy:

$$\mathcal{A}(\underline{u},\underline{u}) = d^3\mathcal{A}_B(\underline{u},\underline{u}) + d\mathcal{A}_M(\underline{u},\underline{u}) + d\mathcal{A}_S(\underline{u},\underline{u}). \tag{2}$$

Here d denotes the thickness of the shell and the different energy components are further given by

$$\begin{aligned}
d^3\mathcal{A}_B(\underline{u},\underline{u}) &= d^3\cdot\int_\Omega\{\nu(\kappa_{11}(\underline{u})+\kappa_{22}(\underline{u}))^2 \\
&\quad +(1-\nu)\sum_{i,j=1}^{2}\kappa_{ij}(\underline{u})^2\}A_1A_2d\alpha_1d\alpha_2 \\
d\mathcal{A}_M(\underline{u},\underline{u}) &= d\cdot 12\int_\Omega\{\nu(\beta_{11}(\underline{u})+\beta_{22}(\underline{u}))^2 \\
&\quad +(1-\nu)\sum_{i,j=1}^{2}\beta_{ij}(\underline{u})^2\}A_1A_2d\alpha_1d\alpha_2 \\
d\mathcal{A}_S(\underline{u},\underline{u}) &= d\cdot 6(1-\nu)\int_\Omega\{\rho_1(\underline{u})^2+\rho_2(\underline{u})^2\}A_1A_2d\alpha_1d\alpha_2.
\end{aligned}$$

where κ_{ij}, β_{ij} and ρ_i denote the bending, membrane and transverse shear strains, respectively, and ν is the Poisson number of the material. The integrals are calculated over the midsurface Ω of the shell which is parametrized by the (generally curvilinear) principal curvature coordinates α_i. The metric of the shell surface is given by the Lamé parameters A_i.

Remark 1 *In some instances it is customary to use the scaled thickness $t = d/L$ where L denotes the characteristic length of the shell. However, in the cases under study L equals unity and therefore we may take $t = d$ for any practical purposes.*

Remark 2 *In our model we have omitted the constant factor $D = \frac{E}{12(1-\nu^2)}$, where E is the Young modulus of the material, from the energy expressions. Consequently, all the results can be considered to be scaled with a factor D^{-1}.*

The strains are taken to be [2]

$$\begin{aligned}
\beta_{11} &= \frac{1}{A_1}\frac{\partial u}{\partial\alpha_1}+\frac{v}{A_1A_2}\frac{\partial A_1}{\partial\alpha_2}+\frac{w}{R_1} \\
\beta_{22} &= \frac{1}{A_2}\frac{\partial v}{\partial\alpha_2}+\frac{u}{A_1A_2}\frac{\partial A_2}{\partial\alpha_1}+\frac{w}{R_2} \\
\beta_{12} &= \frac{1}{2}(\frac{1}{A_1}\frac{\partial v}{\partial\alpha_1}+\frac{1}{A_2}\frac{\partial u}{\partial\alpha_2}-\frac{u}{A_1A_2}\frac{\partial A_1}{\partial\alpha_2}-\frac{v}{A_1A_2}\frac{\partial A_2}{\partial\alpha_1}) = \beta_{21}
\end{aligned}$$

$$
\begin{aligned}
\kappa_{11} &= \frac{1}{A_1}\frac{\partial\theta}{\partial\alpha_1} + \frac{\psi}{A_1A_2}\frac{\partial A_2}{\partial\alpha_2} \\
\kappa_{22} &= \frac{1}{A_2}\frac{\partial\psi}{\partial\alpha_2} + \frac{\theta}{A_1A_2}\frac{\partial A_2}{\partial\alpha_1} \\
\kappa_{12} &= \frac{1}{2}[\frac{1}{A_1}\frac{\partial\psi}{\partial\alpha_1} + \frac{1}{A_2}\frac{\partial\theta}{\partial\alpha_2} - \frac{\theta}{A_1A_2}\frac{\partial A_1}{\partial\alpha_2} - \frac{\psi}{A_1A_2}\frac{\partial A_2}{\partial\alpha_1} \\
&\quad -\frac{1}{R_1}(\frac{1}{A_1}\frac{\partial u}{\partial\alpha_2} - \frac{v}{A_1A_2}\frac{\partial A_2}{\partial\alpha_1}) \\
&\quad -\frac{1}{R_2}(\frac{1}{A_1}\frac{\partial v}{\partial\alpha_1} - \frac{u}{A_1A_2}\frac{\partial A_1}{\partial\alpha_2})] = \kappa_{21}
\end{aligned}
$$

and

$$
\begin{aligned}
\rho_1 &= \frac{1}{A_1}\frac{\partial w}{\partial\alpha_1} - \frac{u}{R_1} - \theta \\
\rho_2 &= \frac{1}{A_2}\frac{\partial w}{\partial\alpha_2} - \frac{v}{R_2} - \psi
\end{aligned}
$$

where the R_i's are the principal radii of curvature of the shell at the point (α_1, α_2).

Given an energy space $\mathcal{U} \subset [H^1(\Omega)]^5$ the above definitions lead to a variational formulation: Find $\underline{u} \in \mathcal{U}$ s.t.

$$
\mathcal{A}(\underline{u}, \underline{v}) = Q(\underline{v}) \quad \forall \underline{v} \in \mathcal{U} \tag{3}
$$

and further to a conforming finite-element approximation in a finite-dimensional subspace $\mathcal{U}_h \subset \mathcal{U}$: Find $\underline{u}_h \in \mathcal{U}_h$ s.t.

$$
\mathcal{A}(\underline{u}_h, \underline{v}) = Q(\underline{v}) \quad \forall \underline{v} \in \mathcal{U}_h \tag{4}
$$

3 The Benchmark Cases

For shells of revolution we note that the entire geometry of the problem is defined by a profile function Φ and the axis of revolution. In this paper we consider the case when the axis of revolution is the x-axis and the profile function is given by $\Phi = \Phi(x) > 0$, $x \in [-L, L]$ for some $L > 0$. Thus, the profile function Φ gives the radius of the shell at the point x. In this case the coordinates α_1 and α_2 correspond to the x-coordinate and the angle of rotation denoted by y, respectively. Further, the Lamé parameters depend only on x and are given by

$$
A_1(x) = \sqrt{1 + [\Phi'(x)]^2}, \quad A_2(x) = \Phi(x), \tag{5}
$$

and the radii of curvature satisfy

$$
R_1(x) = -\frac{[A_1(x)]^3}{\Phi''(x)}, \quad R_2(x) = A_1(x)A_2(x) \tag{6}
$$

For benchmarking purposes the variational problem (3) can be reduced to a one-dimensional problem. Firstly, we assume that the load acting on the shell is a pressure load, i.e.

$$Q(\underline{u}) = \int_\Omega f(x,y)w(x,y)dxdy. \tag{7}$$

Secondly, we assume that the load is periodic in the angular variable and given by

$$f(x,y) = P(x)\cos(\lambda y). \tag{8}$$

For $\lambda \neq 1$ the load given by (7), (8) is self-balancing and thus orthogonal to any rigid body modes that may arise.

The assumptions (7), (8) imply that the solution is given by

$$\underline{u}(x,y) = \begin{pmatrix} u(x)\cos(\lambda y) \\ v(x)\sin(\lambda y) \\ w(x)\cos(\lambda y) \\ \theta(x)\cos(\lambda y) \\ \psi(x)\sin(\lambda y) \end{pmatrix} \tag{9}$$

Substituting the load (7), (8) and the Ansatz (9) into the variational formulation (3) and integrating with respect to the angular variable y we end up with a one-dimensional problem: Find $\underline{u} = (u(x), v(x), w(x), \theta(x), \psi(x)) \in \mathcal{U}$ s.t.

$$\mathcal{A}(\underline{u},\underline{v}) = d^3\mathcal{A}_B(\underline{u},\underline{v}) + d\mathcal{A}_M(\underline{u},\underline{v}) + d\mathcal{A}_S(\underline{u},\underline{v}) = Q(\underline{v}) \quad \forall \underline{v} \in \mathcal{U} \tag{10}$$

where $\mathcal{U} \subset H^1(-L,L)$ is the one-dimensional energy space. In (10) the bending, membrane and shear energies are given by

$$\begin{aligned}
d^3\mathcal{A}_B(\underline{u},\underline{u}) &= d^3 \cdot \pi \int_{-L}^{L} \{\nu(\kappa_{11}(\underline{u}) + \kappa_{22}(\underline{u}))^2 \\
&\quad + (1-\nu)\sum_{i,j=1}^{2} \kappa_{ij}(\underline{u})^2\} A_1 A_2 dx \\
d\mathcal{A}_M(\underline{u},\underline{u}) &= d \cdot 12\,\pi \int_{-L}^{L} \{\nu(\beta_{11}(\underline{u}) + \beta_{22}(\underline{u}))^2 \\
&\quad + (1-\nu)\sum_{i,j=1}^{2} \beta_{ij}(\underline{u})^2\} A_1 A_2 dx \\
d\mathcal{A}_S(\underline{u},\underline{u}) &= d \cdot 6(1-\nu)\,\pi \int_{-L}^{L} \{\rho_1(\underline{u})^2 + \rho_2(\underline{u})^2\} A_1 A_2 dx.
\end{aligned}$$

and the load by

$$Q(\underline{v}) = \pi \int_{-L}^{L} P(x)w(x)dx \tag{11}$$

The one-dimensional strains are in this case given by

$$\begin{aligned}
\beta_{11} &= \frac{1}{A_1}\frac{\partial u}{\partial x} + \frac{w}{R_1} \\
\beta_{22} &= \frac{1}{A_2}\lambda v + \frac{u}{A_1 A_2}\frac{\partial A_2}{\partial x} + \frac{w}{R_2} \\
\beta_{12} &= \frac{1}{2}\left(\frac{1}{A_1}\frac{\partial v}{\partial x} + \frac{1}{A_2}(-\lambda)u - \frac{v}{A_1 A_2}\frac{\partial A_2}{\partial x}\right) = \beta_{21}
\end{aligned}$$

$$\begin{aligned}
\kappa_{11} &= \frac{1}{A_1}\frac{\partial \theta}{\partial x} \\
\kappa_{22} &= \frac{1}{A_2}\lambda\psi + \frac{\theta}{A_1 A_2}\frac{\partial A_2}{\partial x} \\
\kappa_{12} &= \frac{1}{2}\Big[\frac{1}{A_1}\frac{\partial \psi}{\partial x} + \frac{1}{A_2}(-\lambda)\theta - \frac{\psi}{A_1 A_2}\frac{\partial A_2}{\partial x} \\
&\quad -\frac{1}{R_1}\left(\frac{1}{A_1}(-\lambda)u - \frac{v}{A_1 A_2}\frac{\partial A_2}{\partial x}\right) \\
&\quad -\frac{1}{R_2}\left(\frac{1}{A_1}\frac{\partial v}{\partial x}\right)\Big] = \kappa_{21}
\end{aligned}$$

and

$$\begin{aligned}
\rho_1 &= \frac{1}{A_1}\frac{\partial w}{\partial x} - \frac{u}{R_1} - \theta \\
\rho_2 &= \frac{1}{A_2}(-\lambda)w - \frac{v}{R_2} - \psi
\end{aligned}$$

The one dimensional variational formulation (10) is then solved by a high-order finite-element method in an overkill manner to produce accurate reference results. From the solution $\underline{u}_h = (u_h(x), v_h(x), w_h(x), \theta_h(x), \psi_h(x))$ the approximate two-dimensional fields can be reconstructed as per (9).

Remark 3 *We note that the one dimensional fields are also solutions to the Euler equations given by*

$$
\begin{aligned}
&d^3\cdot(1-\nu)\kappa_{12}\frac{(-\lambda)}{R_1A_1}+d\cdot 12\Big[-\frac{\partial}{\partial x}(\beta_{11}\frac{1}{A_1}+\beta_{22}\frac{\nu}{A_1})+\\
&(\nu\beta_{11}+\beta_{22})\frac{1}{A_1A_2}\frac{\partial A_2}{\partial x}+\beta_{12}\frac{\lambda}{A_2}\Big]-d\cdot 6(1-\nu)\rho_1\frac{1}{R_1}=0,\\
&d^3\cdot(1-\nu)\Big[\frac{\partial}{\partial x}(\kappa_{12}\frac{1}{R_2A_1})+\kappa_{12}\frac{1}{A_1A_2}\frac{\partial A_2}{\partial x}\Big]\\
&+d\cdot 12\Big[(\nu\beta_{11}+\beta_{22})\frac{(-\lambda)}{A_2}-\frac{\partial}{\partial x}(\beta_{12}\frac{1}{A_1})-\beta_{12}\frac{1}{A_1A_2}\frac{\partial A_2}{\partial x}\Big]\\
&-d\cdot 6(1-\nu)\rho_2\frac{1}{R_2}=0,\\
&d\cdot 12\Big[\beta_{11}(\frac{1}{R_1}+\frac{\nu}{R_2})+\beta_{22}(\frac{1}{R_2}+\frac{\nu}{R_1})\Big]\\
&+d\cdot 6(1-\nu)\Big[-\frac{\partial}{\partial x}(\rho_1\frac{1}{A_1})+\rho_2\frac{\lambda}{A_2}\Big]=P(x),\\
&d^3\cdot\Big[-\frac{\partial}{\partial x}(\kappa_{11}\frac{1}{A_1}+\kappa_{22}\frac{\nu}{A_1})+(\nu\kappa_{11}+\kappa_{22})\frac{1}{A_1A_2}\frac{\partial A_2}{\partial x}+(1-\nu)\kappa_{12}\frac{\lambda}{A_2}\Big]\\
&-d\cdot 6(1-\nu)\rho_1=0,\\
&d^3\cdot\Big[(\nu\kappa_{11}+\kappa_{22})\frac{-\lambda}{A_2}+(1-\nu)(-\frac{\partial}{\partial x}(\kappa_{12}\frac{1}{A_1})-\kappa_{12}\frac{1}{A_1A_2}\frac{\partial A_2}{\partial x})\Big]\\
&-d\cdot 6(1-\nu)\rho_2=0
\end{aligned}
$$

and the constants of integration are determined by the boundary conditions.

In order to obtain a relatively simple but yet interesting benchmark problem a profile function

$$\Phi(x)=1+\alpha x^2,\quad x\in[-L,L] \tag{12}$$

with $L=1$ and $-1/2\le\alpha\le 1/2$ is chosen. With this choice the cases $\alpha>0$ correspond to hyperbolic shells whereas the cases $\alpha<0$ lead to elliptic geometries. The choice $\alpha=0$ gives the parabolic case (i.e. a cylinder) and is not of interest here. In addition, for each geometry, three different boundary conditions are considered:

1. Clamped boundary, i.e. $\underline{u}(-1)=\underline{u}(1)=0$.
2. Free boundary, no constraints imposed at $x=\pm 1$.
3. Sliding support, i.e. $w(-1)=w(1)=0$ but no other constraints at $x=\pm 1$

The reason for these three choices is that the first conditions leads to membrane-dominated deformation states where no inextensional deformations exist and

the second condition with suitable loading falls into the category of bending-dominated deformation states. In the third case a strong boundary layer typically appears.

The load acting on the shell surface is taken to be a constant pressure load, i.e. $P(x) = P_0$ in (8).

4 Results

In our model the load is not scaled in the thickness d. This results in energies tending to infinity as $d \to 0$. Therefore it is sensible to scale the energies and deformation fields with proper exponent of d. It turns out that in case of a clamped boundary the scaling factor d is appropriate, in case of a free boundary the exponent d^3 naturally appears, and in case of sliding support the factor $d^{3/2}$ gives nicely bounded energies.

In the numerical computations the parameters are chosen as follows: $P_0 = 1$, $\lambda = 2$, and $\nu = 1/3$. Further, the values of α are chosen to be $\alpha = -1/2$ for the elliptic case and $\alpha = 1/2$ for the hyperbolic case.

4.1 Deformation fields

The w-component of the deformation field for the elliptic case is shown in Fig. 1 and for the hyperbolic case in Fig. 2 for each of the three boundary conditions and for the thickness $d = 0.01$.

4.2 Energy distributions

The values of different energy components for an elliptic and a hyperbolic shell is shown in Tables 1 – 3. As expected, the deformation energy is mainly due to membrane energy in case of a clamped boundary whereas in case of a free boundary bending energy dominates. The third boundary condition considered, the case of a sliding support, leads to a mixed configuration where the membrane energy is roughly three or four times the bending energy. It should be noted that the contribution of the shear energy is in general negligible for the type of load applied.

4.3 Boundary layers

It is predicted theoretically that in both cases, elliptic and hyperbolic, boundary layers of length $1/d$ and $1/\sqrt{d}$ appear [4]. These are very well visible in Figures 3 and 4 where three different values of d are plotted together in a close up near the other end-point $x = 1$. Also, the amplitudes are scaled by a power of d in addition to the basic scaling introduced at the beginning of section 4.

Note that the $1/d$ layer is not present if the Kirchhoff model is used, i.e. if the shear strains are assumed to vanish and consequently the energy component associated with this short layer is of negligible size.

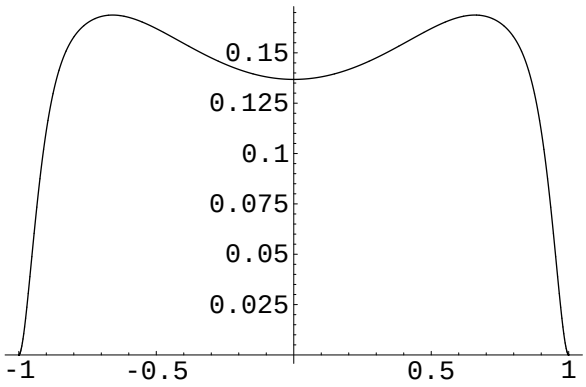

(a) Elliptic shell, clamped boundary, scaling factor d.

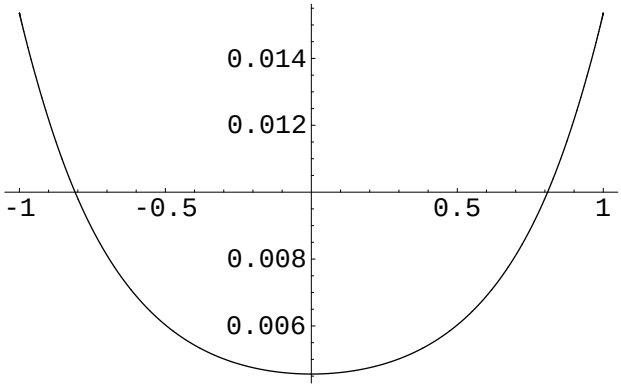

(b) Elliptic shell, free boundary, scaling factor d^3.

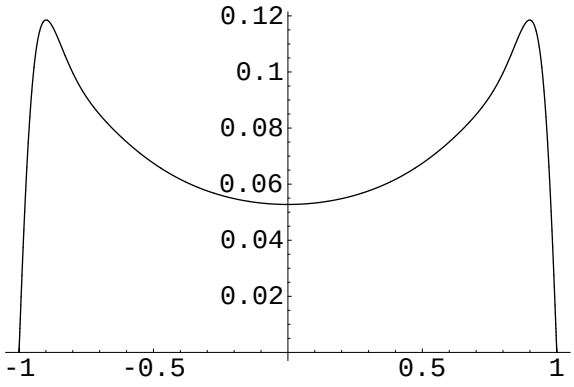

(c) Elliptic shell, sliding support, scaling factor $d^{3/2}$.

Figure 1: Deformation profiles of elliptic benchmark shells with $\alpha = -1/2$ and $d = 0.01$.

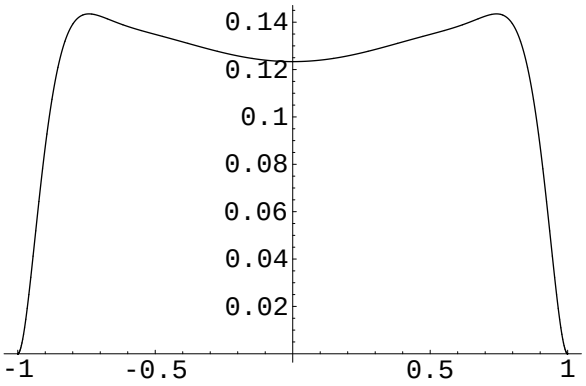

(a) Hyperbolic shell, clamped boundary, scaling factor d.

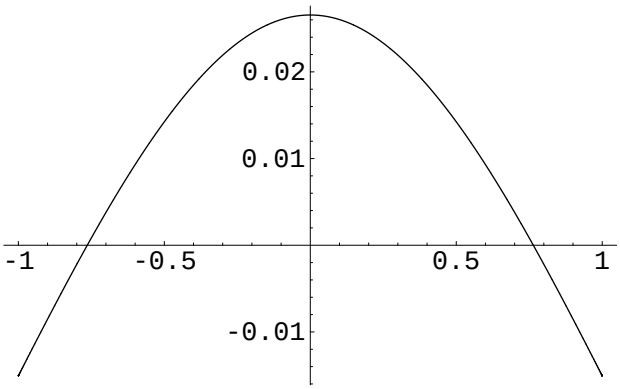

(b) Hyperbolic shell, free boundary, scaling factor d^3.

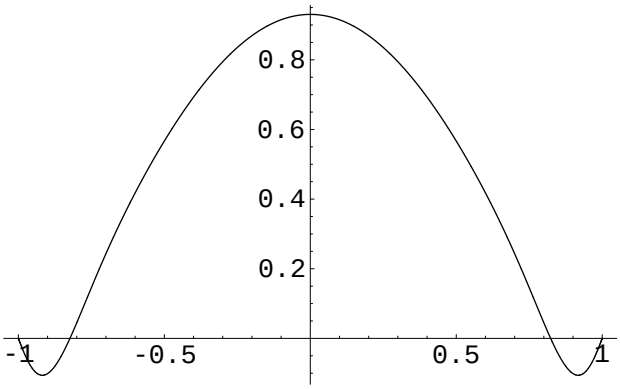

(c) Hyperbolic shell, sliding support, scaling factor $d^{3/2}$.

Figure 2: Deformation profiles of hyperbolic benchmark shells with $\alpha = 1/2$ and $d = 0.01$.

Table 1: Bending and membrane deformation energies of the elliptic benchmark shell with $\alpha = -1/2$ for different boundary conditions and thickness.

bc	scaling	d	bending	membrane
clamped	d	0.1	0.067932274375052329846	0.6529083197266562495
clamped	d	0.01	0.0103830463685097923	0.882496248727063182
clamped	d	0.001	0.00125738437054832597	0.911085652488554903
free	d^3	0.1	0.05259865416361741899	0.016340716502303697963
free	d^3	0.01	0.04482455416706005	0.000518711236301804
free	d^3	0.001	0.0445615374485630	0.00000910669449100
sliding	$d^{3/2}$	0.1	0.121531656841800993	0.376653195459904178
sliding	$d^{3/2}$	0.01	0.10023313105636776	0.35255544437330241
sliding	$d^{3/2}$	0.001	0.097760476060097	0.3146453371291655

Table 2: Bending and membrane deformation energies of the hyperbolic benchmark shell with $\alpha = 1/2$ for different boundary conditions and thickness.

bc	scaling	d	bending	membrane
clamped	d	0.1	0.0503943539707896942	0.5898711230384374474
clamped	d	0.01	0.012885686264982638	0.75063903767235717
clamped	d	0.001	0.003945073398564912	0.79448479732357318
free	d^3	0.1	0.07345043843274972	0.0454278042763258840
free	d^3	0.01	0.07096148230262519	0.00050691514487500
free	d^3	0.001	0.070928877870723	0.000005675569089ă
sliding	$d^{3/2}$	0.1	1.6172362524993354	2.019491461183940693
sliding	$d^{3/2}$	0.01	0.4512398801411733	2.6183584078606343
sliding	$d^{3/2}$	0.001	0.429359677890091	1.724365800207987

Table 3: Shear deformation energies of the elliptic and hyperbolic benchmark shells with $\alpha = \pm 1/2$ for different boundary conditions and thickness.

bc	scaling	d	shear (elliptic)	shear (hyperbolic)
clamped	d	0.1	0.0141326720498383618	0.00488440125780130
clamped	d	0.01	0.00021889131306770	0.00014965245645691
clamped	d	0.001	0.000003415112101626	0.000004572518992731
free	d^3	0.1	0.003059859817461312484	0.00140478553416503418
free	d^3	0.01	0.0001950685145649701 6	0.00004217225656242
free	d^3	0.001	0.0000186715544510	0.00000321135199450
sliding	$d^{3/2}$	0.1	0.01728331306404600426	0.03101233723801069
sliding	$d^{3/2}$	0.01	0.00139067900641246	0.0017604214947907
sliding	$d^{3/2}$	0.001	0.0001227384878609	0.0001755007710594

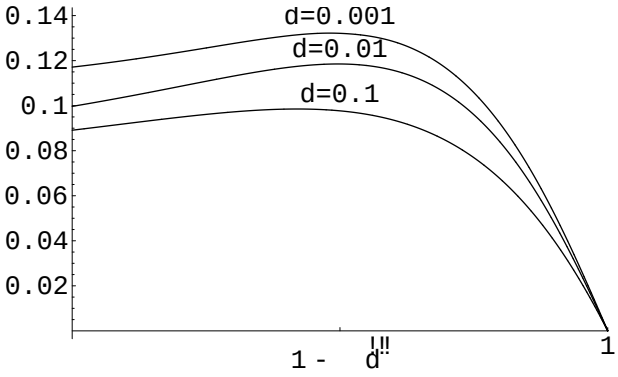

(a) Elliptic shell, sliding support, $1/\sqrt{d}$-layer in w-component.

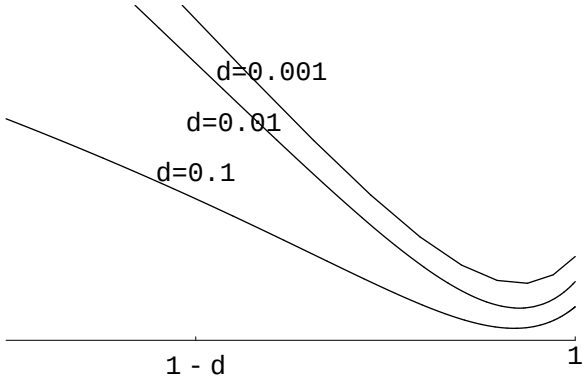

(b) Elliptic shell, free boundary, $1/d$-layer in ψ-component, scaling factor $1/d$.

Figure 3: The $1/\sqrt{d}$- and $1/d$-scale boundary layers in the elliptic shell.

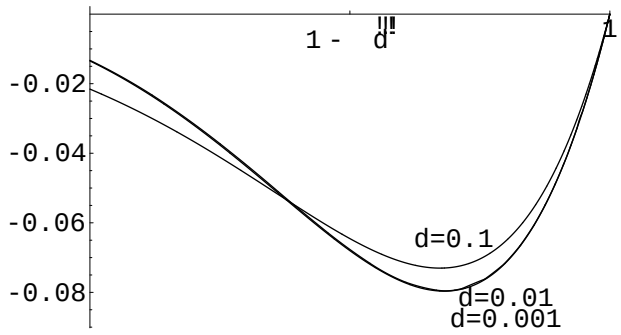

(a) Hyperbolic shell, clamped boundary, $1/\sqrt{d}$-layer in θ-component, scaling factor $\sqrt{d}$.

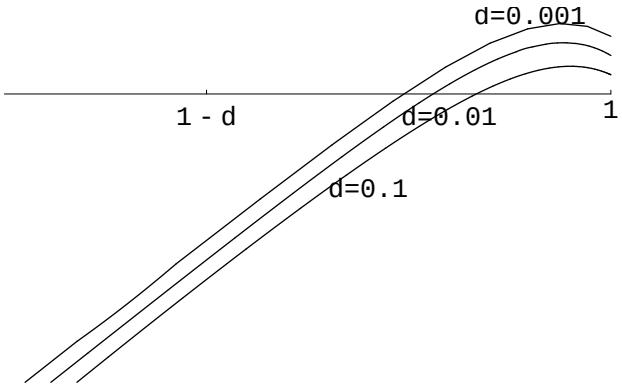

(b) Hyperbolic shell, free boundary, $1/d$-layer in ψ-component, scaling factor $1/d$.

Figure 4: The $1/\sqrt{d}$- and $1/d$-scale boundary layers in the hyperbolic shell.

5 Conclusions

Shells of revolution provide a good basis also for benchmarking hyperbolic and elliptic shell geometries. Suitably selected load allows to reduce the dimension of problem by one allowing an accurate solution of the deformation fields.

The benchmark cases considered strengthen several principal ideas on the behaviour of thin hyperbolic and elliptic shells when using the model of Reissner and Naghdi:

1. The deformation state can be either bending- or membrane-dominated – or some intermediate state. Constraints imposed on the boundary have a great impact on the actual deformation state.

2. The contribution of the transverse shear energy is typically negligible.

3. Boundary layers of scales $1/d$ and $1/\sqrt{d}$ appear.

However, considering only basic benchmark cases like the ones in the present paper would give too narrow a vision on the very rich garden of differently behaving shell structures. Therefore, in a forthcoming paper we shall analyse a sensitive shell that is intended to shed light on more complex aspects of shell modelling.

References

[1] K.-J.Bathe, A.Iosilevich and D.Chapelle, An evaluation of the MITC shell elements. *Computers & Structures* **75** (2000), no. 1, 1–30.

[2] M. Malinen, On the classical shell model underlying bilinear degenerated shell finite elements: general shell geometry. *Internat. J. Numer. Methods Engrg.* **55** (2002), no. 6, 629–652.

[3] J.Pitkäranta, Y.Leino, O.Ovaskainen and J.Piila, Shell deformation states and the finite element method: a benchmark study of cylindrical shells. *Comput. Methods Appl. Mech. Engrg.* **128** (1995), no. 1-2, 81–121.

[4] J. Pitkäranta, A.-M. Matache, C. Schwab, Fourier mode analysis of layers in shallow shell deformations. *Seminar für Angewandte Mathematik, Eidgenössische Technische Hochschule*, Research Report No. 99-18 (1999)

(continued from the back cover)

A449 Juhani Pitkäranta
Mathematical and historical reflections on the lowest order finite element models for thin structures
May 2002

A448 Teijo Arponen
Numerical solution and structural analysis of differential-algebraic equations
May 2002

A447 Timo Salin
Quenching-rate estimate for a reaction diffusion equation with weakly singular reaction term
April 2002

A446 Tuomas Hytönen
R-Boundedness is Necessary for Multipliers on H^1
February 2002

A445 Philippe Clment , Stig-Olof Londen , Gieri Simonett
Quasilinear Evolutionary Equations and Continuous Interpolation Spaces
March 2002

A444 Tuomas Hytönen
Convolutions, Multipliers and Maximal Regularity on Vector-Valued Hardy Spaces
December 2001

A443 Tuomas Hytönen
Existence and Regularity of Solutions of the Korteweg - de Vries Equations and Generalizations
December 2001

A442 Ville Havu
Analysis of Reduced Finite Element Schemes in Parameter Dependent Elliptic Problems
December 2001

A441 Jukka Liukkonen
Data Reduction and Domain Truncation in Electromagnetic Obstacle Scattering
October 2001

A440 Ville Turunen
Pseudodifferential calculus on compact Lie groups and homogeneous spaces
September 2001

HELSINKI UNIVERSITY OF TECHNOLOGY INSTITUTE OF MATHEMATICS
RESEARCH REPORTS

The list of reports is continued inside. Electronical versions of the reports are available at *http://www.math.hut.fi/reports/* .

A454 Timo Eirola , Marko Huhtanen , Jan von Pfaler
Solution methods for R-linear problems in C^n
October 2002

A453 Marko Huhtanen
Aspects of nonnormality for iterative methods
September 2002

A452 Kalle Mikkola
Infinite-Dimensional Linear Systems, Optimal Control and Algebraic Riccati Equations
October 2002

A451 Marko Huhtanen
Combining normality with the FFT techniques
September 2002

A450 Nikolai Yu. Bakaev
Resolvent estimates of elliptic differential and finite element operators in pairs of function spaces
August 2002

ISBN 951-22-6315-7
ISSN 0784-3143